



## Controlling fatigue crack paths for crack surface marking and growth investigations

S. Barter, P. White, M. Burchill

*Aerospace Division, Defence Science and Technology Organisation, Australia*

*Simon.Barter@dsto.defence.gov.au, Paul.White@dsto.defence.gov.au, Madeleine.Burchill@dsto.defence.gov.au.*

**Abstract.** While it is well known that fatigue crack growth in metals that display confined slip, such as high strength aluminium alloys, develop crack paths that are responsive to the loading direction and the local microstructural orientation, it is less well known that such paths are also responsive to the loading history. In these materials, certain loading sequences can produce highly directional slip bands ahead of the crack tip and by adjusting the sequence of loads, distinct fracture surface features or progression marks, even at very small crack depths can result. Investigating the path a crack selects in fatigue testing when particular combinations of constant and variable amplitude load sequences are applied is providing insight into crack growth. Further, it is possible to design load sequences that allow very small amounts of crack growth to be measured, at very small crack sizes, well below the conventional crack growth threshold in the aluminium alloy discussed here.

This paper reports on observations of the crack path phenomenon and a novel test loading method for measuring crack growth rates for very small crack depths in aluminium alloy 7050-T7451 (an important aircraft primary structural material). The aim of this work was to firstly generate short- crack constant amplitude growth data and secondly, through the careful manipulation of the applied loading, to achieve a greater understanding of the mechanisms of fatigue crack growth in the material being investigated. A particular focus of this work is the identification of the possible sources of crack growth retardation and closure in these small cracks. Interpreting these results suggests a possible mechanism for why small fatigue crack growth through this material under variable amplitude loading is faster than predicted from models based on constant amplitude data alone.

**Keywords.** Fatigue crack growth; Crack closure; Crack paths; Underloads; Variable amplitude; Constant amplitude; Quantitative Fractography, Cyclic stress intensity factor  $\Delta K$ .

### INTRODUCTION

Fatigue crack growth in metals that display localisation of slip, (or confined slip) develop fracture surface morphologies which reveal that crack path changes are not only dependent on the loading direction and the local microstructural orientation of the grains, but also on the loading history. In these materials, certain simple variable amplitude (VA) loading sequences can produce localised plasticity in the form of strong confined slip bands ahead of the crack tip as a result of both the loading and unloading of each load cycle. The interaction of load cycles and crack tip slip bands strongly influences the crack path. As a result of this, it has been found that loading patterns involving sequences with high R (load ratio) cycles followed by either loading cycles with a significantly different R (low R or -R) or segments of VA loads, can often produce distinct fracture surface features or *progression marks*.



Understanding this behaviour provides a researcher with the valuable ability to use loading changes to *steer* the crack front, and has been used here to delineate the crack growth under a desired loading spectrum [1-3]. These path changes are investigated further here for small cracks, and are used in the measurement of crack growth rates at low-to-very low stress intensity ranges ( $\Delta K$ ), and to investigate the influence of load history on local retardation (closure) in such cracks.

## BACKGROUND

The purpose of the work being reported here is to make improvements to current fatigue crack growth models so that better predictions of fatigue life can be made for critical airframe components. Predicting the life of aircraft structural metallic components loaded with VA spectra remains difficult since current methods do not achieve accurate results for crack growth in the small<sup>1</sup> to intermediate size range, which often governs the total fatigue life of a component [4-6]. The influence of small crack growth rates on the total fatigue life can be significant for a typical combat aircraft with a highly stressed structure, where the critical crack sizes are often less than 10mm [7] in depth, at least two thirds of the total fatigue life is consumed when the fatigue cracks are small. Further, the accurate prediction of such small cracks is of interest to aircraft maintainers and operators since it may be used to set inspection intervals, or schedules for repairs and modifications in managing the airframe throughout the service life.

Constant amplitude (CA) crack growth data is the common input for VA fatigue crack growth predictions. For small cracks the data is usually drawn from methods that rely on measuring the incremental changes in the surface length of a crack, rather than its depth [1, 7, 8]. This is thought to introduce considerable scatter [9] into the results as the surface extension of small cracks occurs in a plane stress state - compared to the internal crack tip, which is influenced by plane strain. An additional complication to the prediction of VA crack growth is the influence that spectrum effects can have, such as those produced by large loads. These loads may produce retardation (and/or acceleration) of crack growth, and this is often described in literature as a product of crack tip *closure*, although this and other effects are generally grouped together under the same term [10]. To address these effects, adjustments are typically made to the predictive algorithms to match measured experimental observations i.e. those discussed in [11]. Other influences, such as the environment, may also be present but this is usually addressed, in part, by using data collected in an environment with similar conditions to that of service. Regardless of these adjustments, predictions of natural cracks that have grown from small initial discontinuities remains poor for many of the metallic materials that may be found in aircraft structures. Further, actual growth when cracks are in the small to intermediate range (from tens of microns to several millimetres [12]) is often under predicted, whereas it may be over predicted for intermediate sizes up to failure. Here, some appropriate data and observed crack growth features for small cracks in a selection of specimens, along with suitable adjustments to allow the predictive models to address closure effects amongst other important issues, are briefly discussed.

VA loading sequences are known to produce progression marks on fatigue crack surfaces [1, 13, 14], at growth rates well below those where *striations*<sup>2</sup> can be seen. These marks, for small cracks, are usually associated with either a local change in the crack path that leads to a visible feature on the fracture surface or a change in the fracture surface *texture*. Such a local crack path change may take the form of a relatively prominent ridge, and a corresponding depression on the matching face, where a large change in load amplitude or peak load is/are followed by cycles that are significantly different in range or peak, i.e. with low or negative R [15, 16]. Such features, often have considerable variety, form the markings that are visible on the fracture surface of cracks grown with complex VA loading spectra. However, when such a VA loading sequence is repeated during a fatigue test, these markings may be particularly evident as repeating patterns even at very low crack growth rates. An example of a small crack in aluminium alloy (AA)7050-T7451, the material of interest here, growing away from multiple initiation sites on a surface coated with ion vapour deposited aluminium is shown in Fig. 1, where the repeat of the complex VA spectrum (wing root bending moment in this case) is evident. In this figure, the crack growth bands produced by the repeat of the VA spectrum blocks (containing  $\approx 6000$  cycles) are visible as *progression bands* down to approximately  $1\mu\text{m}$  in width (at higher magnifications [3] smaller progression bands can be measured). This suggests an average crack growth rate of approximately  $10^{-9}$  m/cycle if all the loads cause growth, which for the case of the example shown has been found to be likely due to the growth

<sup>1</sup> The definition of 'small' in this context may be found in [13].

<sup>2</sup> Striations, the result of a single load cycle, can be found down to a width of  $\sim 2 \times 10^{-8}$  m/cycle for aluminium alloys [3]. Progression bands are the result of a series of load cycles (that cannot be individually identified); these multi load cycle sequences can also be seen down to about the same growth increment [3].

rates of small cracks being faster and having lower thresholds than long cracks, as will be shown. From this figure, it is clear that part of the reason that these bands are visible is that during the application of a spectrum block the fatigue crack path is changing while the fracture surface texture from each spectrum block is relatively consistent (at this scale).

Path changes produced by load changes have been often observed, particularly with the application of underloads as reported in [16]. Abelkis [19] noted similar features on the fatigue cracks produced in other 7XXX aluminium alloys as well as the 2XXX alloys. Krkoska et al. [21] notes this effect in AA2024-T3, although it was not as strongly defined as found here with AA7050-T7451. From a practical point of view, this leads to one possible method of marking fracture surfaces at growth rates below those where striations are visible: i.e., the use of high R sequences with underloads [3] or sequences with bands of different R.

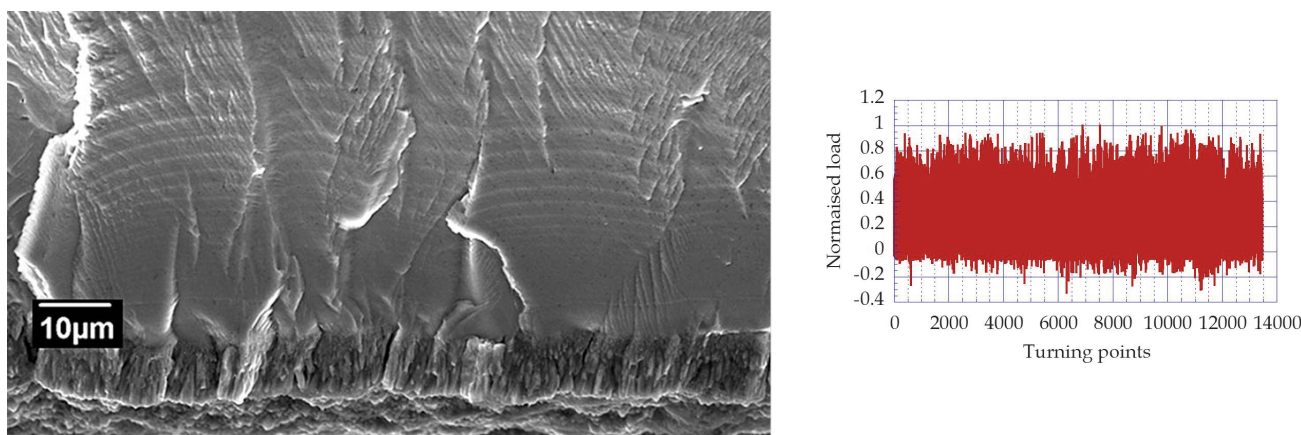


Figure 1: Origin region of cracks grown with repeated applications of the complex wing root bending moment loading sequence shown (left). The cracking started from multiple sites (shallow etch pits) on the ion vapour deposited aluminium coated surface: bottom of the view.

### GENERAL CRACK PATHS IN AA7050-T7451

For stage two fatigue crack growth [15], it is commonly assumed when applying linear elastic fracture mechanics for predictions, that the crack path plane is flat and perpendicular to the loading direction. In this context, *flat* is a relative term since high magnification microscopic examination will usually reveal that this is not the case –roughness is present and this implies that the microscopic crack path is not always perpendicular to the loading direction.

The degree of this path roughness, as the fatigue crack grows, is dependent on: the crack tip stress intensity variation ( $\Delta K$ ) associated with the cyclic loading; the influence of the microstructure; the influence of the environment, etc. [11]. For example, in AA7050-T7451, the surface is generally *faceted* for CA loading where  $\Delta K$  and maximum  $K$  ( $K_{max}$ ) are below  $\sim 5\text{MPa}\sqrt{\text{m}^3}$ . Crack surfaces produced by such loading are shown in Fig. 2A and B that were produced with very simple spectra approximating CA since they consisted of large blocks of CA of  $R=0.5$  with occasional single loads of a different R. (Fig. 2A was taken at a high angle of tilt to highlight the meandering faceted growth of the crack and Fig. 2B was imaged in the scanning electron microscope (SEM) using only one quadrant of the four piece backscatter electron detector to give a shadowed view of the surface: bright facets are tilted towards the detector and dark ones away from the detector). These views clearly indicate that the surfaces are not consistently perpendicular to the loading direction. Additionally, in Fig. 2B, features labelled as *ridges* and *fissures* on the fracture surface, suggest the crack is locally sampling multiple paths around the crack front as it progresses through the material. The *ridges* and *fissures* seen in Fig. 2B coincide with the single low to negative R cycles that were applied occasionally in the  $R=0.5$  loading. The ridges are on the facets *facing* away from the crack origin (the growth direction) and the fissures are on those facets facing the origin and are therefore alternate crack paths.

<sup>3</sup> This is a somewhat arbitrary point and may vary from material to material

At higher  $\Delta K$  and  $K_{max}$  values, the fracture surface appears less crystalline in nature where significant plasticity is evident. In this condition, striations are easily found and the crack growth behaviour at large inclusions (inherent in these materials) are involved in the crack extension and these features influence the crack path. For this reason, the paths taken by fatigue cracks for the two typical regimes; 1)  $\Delta K$  and  $K_{max}$  below  $\sim 5\text{MPa}\sqrt{\text{m}}$ , and 2) above this value to failure, of crack growth have notable differences<sup>4</sup>. While both references [16] discuss striation formation, this paper investigates crack paths in AA7050-T7451 for  $\Delta K_r < 5\text{MPa}\sqrt{\text{m}}$  (growth rates of  $< 2 \times 10^{-7}$  m/cycle), with emphasis on  $\Delta K_r$  less than  $3\text{MPa}\sqrt{\text{m}}$  (growth rates  $< 2 \times 10^{-8}$  m/cycle). This regime includes the transition growth from no striations being observable to striations being easily observed.

Previous work on striation formation can be found in [16]; noting that the explanation in these papers is in some respects at odds with classical descriptions of striation formation such as those found in [17, 18]. The main difference is the observation that matching crack faces appear asymmetric with striation peaks on one face matching striation depressions on the other rather than peak to peak or depression to depression as suggested in the classical descriptions. The observation that the formation of striations is asymmetric does, in-part, explain how changes in loading can produce changes in striation appearance so that with in-completed load cycles the ridges and depressions seen in Fig. 2B are formed rather than completed striations. This has direct implications to crack paths at growth rates below those that result in observable striations.

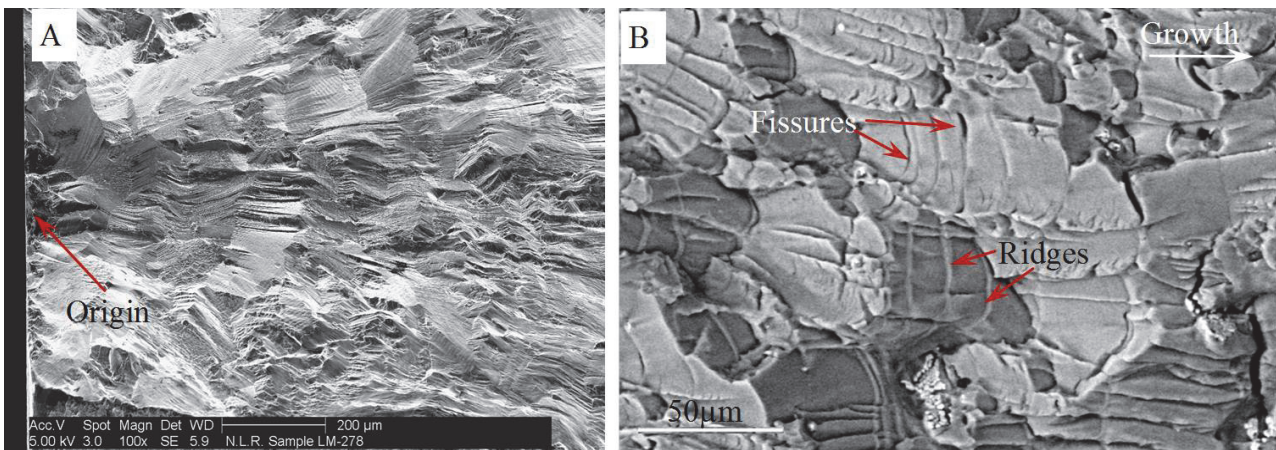


Figure 2: Examples of fatigue crack surfaces produced by simple spectra applied to AA7050-T7451 coupons, showing the macro crack path variation (A) through the crystal structure resulting in a *faceted* fracture surface (taken at a high angle of tilt); and at the micro level (B) with additional features from crack path changes marked (from [15]).

## EXPERIMENTAL METHOD

Simple load sequences were designed with significant variations in  $R$  to investigate a range of crack path deviations. AA7050-T7451 coupons, which were hourglass-shaped, and a low stress concentration were tested to failure in ambient conditions (about  $21^\circ\text{C}$  and humidity 50-70%) with a servo hydraulic fatigue test machine. Various loading sequences were employed, consisting of sub-blocks of VA and CA cycles of various  $R$  and  $\sigma_{max}$  values. To limit retardation effects, the  $\sigma_{max}$  levels were held constant within each test loading sequence. To make the tests physically representative of cracks that may be found in service aircraft structures, the fatigue cracks were grown to failure from small discontinuities approximately  $20\mu\text{m}$  deep, produced by either surface etching or micro laser cutting<sup>5</sup> on the coupon surface. The coupons were all cut from a thick plate with a large effective grain size<sup>6</sup>. After

<sup>4</sup> After striations become obvious in this material it is often found that the crack becomes rougher with obvious intersections with large second phase particles that tend to be to either side of the main growth plane. This results in a different sort of roughness developing. The striations themselves become more plastic (smoother) in appearance although they may show rumpling or slip traces on their flanks and evidence of contact on their leading edges. The secondary paths created by fissures tend to steer parts of the crack front away from the average path and finally the crack path may deviate wildly from the average path and grow in odd local directions due to the involvement of the fissuring and inclusions.

<sup>5</sup> Polished coupons were cut with a regular array of slots by a Coherent Industrial AVIA™ pulsed frequency tripled Nd-YAG LASER operated at

testing, the fatigue cracks were fractographically examined using a field emission gun scanning electron microscope. The crack growth increments, due to the various load sub-blocks, were measured to obtain short crack growth data for comparison with standard  $da/dN$  data for this alloy.

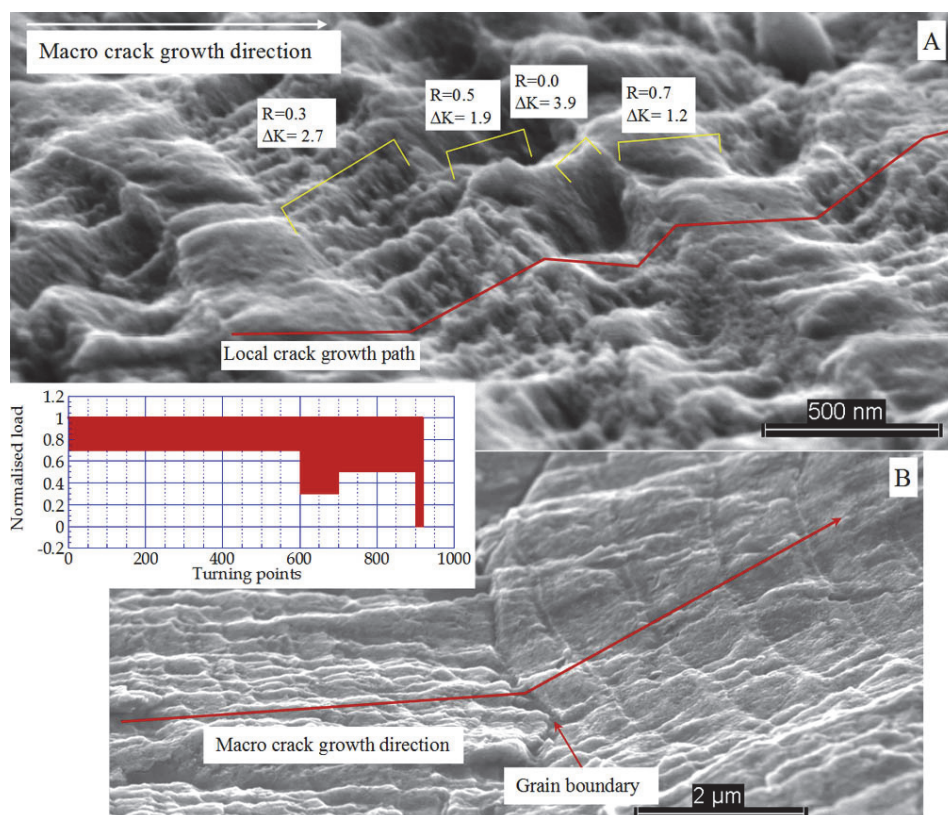


Figure 3: A fatigue crack produced by a simple spectrum (insert) showing the crack path (A) across one grain and (B) two grains. The  $\Delta K$ s for each CA growth bands are marked. Note the morphology and path changes with changing R.

## OBSERVATIONS AND THE DISCUSSION OF CRACK GROWTH IN AA7050-T7451

An example that demonstrates variation in crack growth plane and morphology with load cycles of differing R is given in Fig. 3 for a simple spectrum consisting of four different R CA sub-blocks. In Fig. 3A, the crack path is observed to vary significantly as it progresses through the material. The  $\Delta K$  applicable for each sub-block of crack growth is indicated on the figure. The fatigue crack growth for each CA sub-block of R appears to have a preferred path through this grain, not only changing in orientation or *tilting* in relation to the general crack growth plane, but also *twisting* or rotating about this plane [11]. Of particular note in this figure is the crack growth from the R=0 loading sub-block which appears to have local twisted segments, producing an appearance of deep pockets for its period of growth. In contrast, on the commencement of the R=0.7 loads, these pockets abruptly disappear, although remnants in the form of the well-known *river patterns* persist, on what is then relatively smooth growth. This suggests that in this case the grains orientation is more ideally positioned for R=0.7 crack growth. The net effect of these

---

wavelength of 355nm with a Q-switched (QS) pulse duration of 2μSec, period of 100μSec and a repetition rate of 1KHz.

This produced a 10μm full width half maximum beam at a typical energy of 164μJ/pulse at the position of laser focus. 800 slots were produced by 4 pulses laid next to each other in a row to give slots that were approximately 0.05mm long.

<sup>6</sup> Thick plate AA7050-T7451, that is commonly used to manufacture major aircraft structures, has a large pre-recrystallization grain size from restricted rolling during manufacture. Although the recrystallization grain size may be small (about 10μm), the lack of deformation from the rolling leaves these sub-grains with orientations similar to the pre-recrystallization grains from which they were formed. The fatigue cracking treats these sub-grains as being essentially of the same orientation and results in the large facets seen in many of the coupons tested here, e.g., Fig. 2A.

---

changes is that each CA sub-block appears to have a different preferred growth plane. In trying to achieve this plane, different crack surface *textures* have formed for different Rs, for effectively the same peak  $K_{max}$  (the varies only slightly across this field of view shown).

The extent of the localised tilts and twists of the crack path appear to be highly dependent upon both the crystal orientation and loading interaction, and therefore can be expected to vary from grain-to-grain. This is demonstrated in Fig. 3B where a grain boundary is crossed and a sudden change in the average preferred growth plane occurs. Therefore, as may be expected, the large facets shown in Fig. 3B and in Fig. 2A and B are generally the result of major grain boundary crossings, while the textured surfaces and local paths on these facets are the result of tilts and rotations caused by changes in the loading. As in Fig. 2B, Fig. 3 also shows that the crack at these low  $\Delta K$ s can be considered to be *sampling* various paths – both the preferred planes of the crystal and the unfavourable planes that enable the crack to stay coherent with the average crack front. These features make the cracks growth from individual CA sub- blocks of loading visible at very small  $\Delta K$ s and crack sizes where striations cannot be seen.

A possible explanation for the path changes within a grain is the limited number of slip systems available, since the preferred slip planes and directions will affect the plane of crack extension. Aluminium has a face centred cubic (fcc) crystal structure with 12 primary slip systems: four slip planes and three slip directions for each plane. The activity that occurs on each of these slip systems is key to the paths that the fatigue crack creates at these lower  $\Delta K$ s where plasticity is limited and slip is localised to these planes. Slip occurs on those planes and in those directions that are the easiest to activate given the limited crack driving force, so it is probable that only those planes nearest the planes of maximum shear are activated to progress the crack tip during any load increase. An example of this effect is illustrated in Fig. 4, where the slip bands on the surface of a specimen were produced by large  $\Delta K$  -R cycles in a (mostly +R) VA spectrum for fatigue cracks grown from laser slots. Although the primary slip planes are likely to be those nearest to the maximum shear planes ahead of the crack tip (as is shown in Fig. 4A), they need not be at the 45°, as shown in Fig. 4B, and so the path taken though any one grain will be different from grain to grain. Further, in AA7050-T7451, the formation of this localised slip is very much influenced by the environment, as it is with most aluminium alloys since the presence of hydrogen from the dissociation<sup>7</sup> of water appears to promote the formation of localised slip bands, restricting the plasticity in addition to the microstructural hardening precipitates.

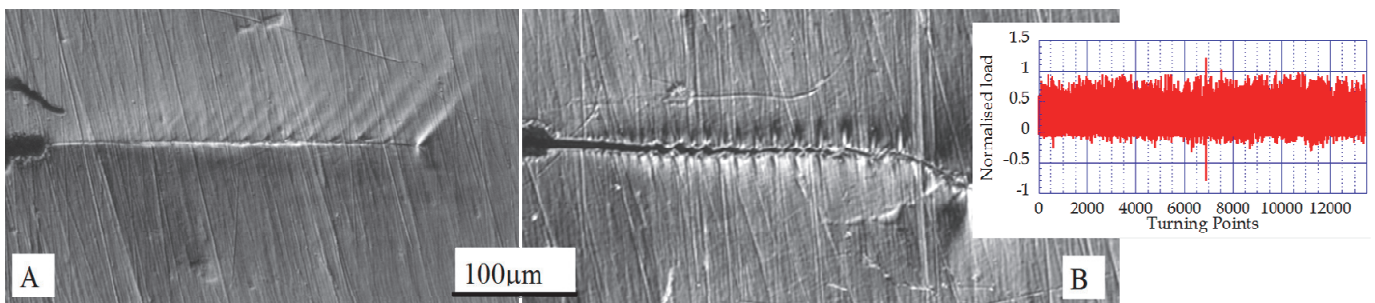


Figure 4: View of two cracks extending from laser slots on the surface of the same specimen showing the slip bands on the primary slip systems in a single grain in each case. They were formed by the peak load in the complex spectrum shown in the insert. Note their asymmetry. Loading was in the vertical direction. (Optical interference contrast images).

Further complicating matters, in 3D an embedded thumbnail shaped fatigue crack will have multiple slip planes each with three slip directions around a curved crack front *and* the shear plane produced by both the loading and un-loading part of the cycle. These will interact differently with these many active slip planes depending upon the micro and macro crack orientation to these to the growth direction<sup>8</sup>. Therefore, it is reasonable to assume that the crack path will also tend to vary about the crack front in a single grain, providing a large number of possible micro and macro growth paths. All of which results in different micro crack paths developing about the crack front and the local front breaking-up and re-forming from location to location about the front. An example of a fatigue crack fracture surface produced by a VA (combat aircraft wing root bending moment) test spectrum with a single 20% overload is shown in Fig. 5. In this figure, the result of the crack front breaking-up due to forced non-ideal growth paths in some regions can be seen though an increase in roughness on the surface due to the crack front parting and re-forming

<sup>7</sup> The influence of hydrogen on the fatigue process in aluminium alloys is an area of debate that will not be further discussed here although strain localisation due to the presence of hydrogen has been proposed [22].

<sup>8</sup> Suggesting that the processes for crack extension at this very small scale maybe similar to the process of striation formation [16].

to remain coherent; Locations A and B. This has led to river-patterns on fatigue crack surfaces that can be compared to the relatively smoother fracture surface labelled at C.

Such local roughness and break-up of the crack front is expected to lead to non-ideal conditions of crack growth. Crack deflection is known to cause slower crack growth, particularly in this material when  $\Delta K$  and  $K_{max} > \sim 5\text{MPa}\sqrt{\text{m}}$ , and bifurcation of the crack appears to occur though fissuring. These are all recognised sources [23] of crack growth retardation, and may indicate a correlation between the extent of deviation from the ideal crack growth path (i.e. roughness) and a decrease in the effective crack opening or  $\Delta K$  (i.e. an increase in the level of closure). In a practical sense, this is important to the question of using CA data to predict VA growth since it has been noted that a VA spectrum results in a smoother and less tortuous crack fracture surface, suggesting a less bifurcated crack path and thus more efficient crack growth. This is demonstrated by comparing the fatigue crack fracture surface in Fig. 6, generated by a test spectrum with sub-blocks of high R CA with underloads, with that shown in Fig. 5. Fig. 6 shows a fracture surface that is far more tortuous with many river patterns on a micro scale that are being significantly influenced by the microstructure of the grains through which the crack is passing, as well as at grain boundaries. This figure also shows that the path taken across each grain and the roughness produced is consistent across that grain suggesting that the crack is becoming locked onto particular sets of paths in each grain for each direction of crack growth. Because the overall crack growth rate is controlled by the average growth through the material, the wide extent of roughness, though the multiple paths being taken, will lead to further retardation of the growth. This can be seen in the more *smooth* growth at location C in Fig. 5, compared to the growth at locations A and B. This is illustrated in the following examination of growth rates.

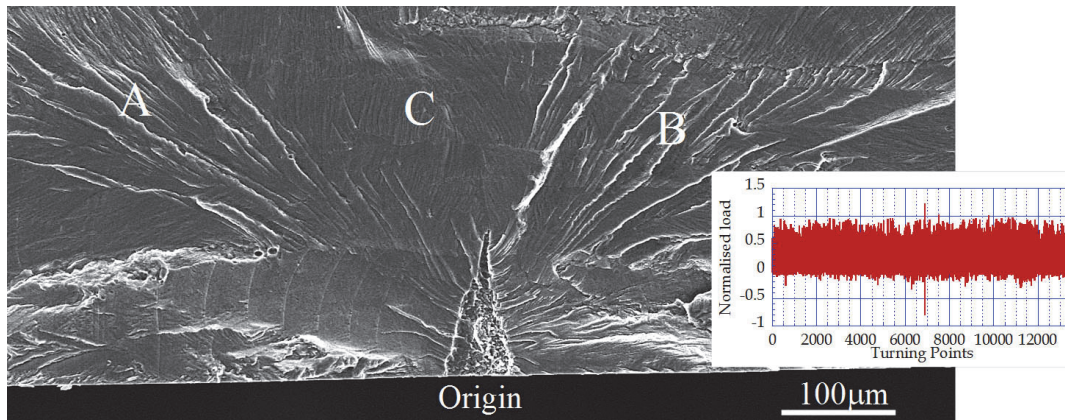


Figure 5: An AA7050-T7451 fatigue crack surface produced by a complex spectrum showing a crack path that is reasonably flat compared to that seen in Fig. 2. While microstructural influence is still obvious it is not as significant as in Fig. 2A. Nevertheless, there are still variations in the conformity of the crack front as it passes through each grain; c.f. regions A and B, where the crack has formed inter planar steps (river patterns) compared to region C which is relatively flat.

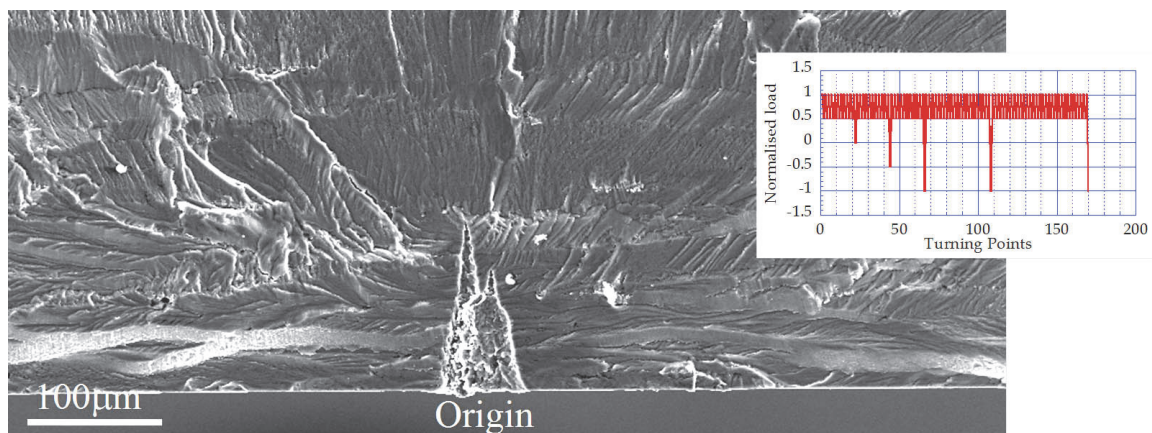


Figure 6: An AA7050-T7451 fatigue crack surface produced by a simple spectrum showing a more crystallographic crack path with many fine changes in direction as the crack attempts to stay aligned to particular planes within each grain of the material.

### PATH EFFECTS ON CRACK GROWTH RATE

The apparent retardation effect that builds up for CA loading, as discussed for Fig. 6, was examined by taking crack growth measurements of short sub-blocks of CA embedded between VA loads. The coupons were tested with CA sub-blocks of: 500, 1000, 2000, 5000 or 10000 cycles; an example of one of these spectra is shown in Fig. 7. In Fig. 7A, a single 10000 cycle sub-block is shown, and it appears to roughen as CA cycles progress; apparently due to a multitude of alternate crack paths being sampled locally by the crack front. The inclusion of VA sub-blocks allowed the measurement of the CA bands due to the notable change in the crack path and morphology of the crack surface between them and the CA sub-blocks, i.e. Fig. 7B and Fig. 8A. Generally, it was found that the CA sub-blocks produced notably rougher surfaces (Fig. 7A) than the VA sub-blocks (Fig. 7B shows clear progression bands that were approximately perpendicular to the loading axis and relatively flat). The change in plane often seen with the CA sub-blocks compared to the VA sub-blocks is shown in Fig. 8A.

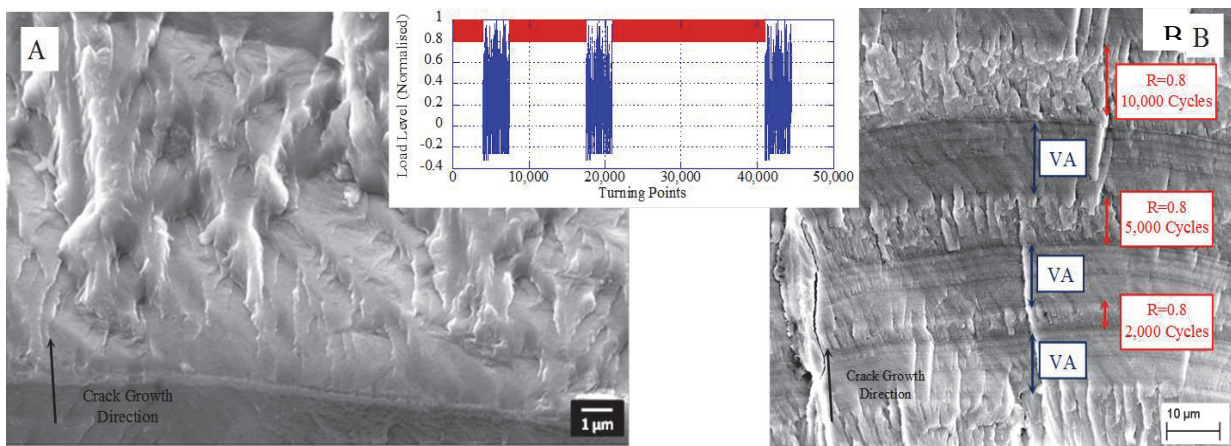


Figure 7: Local detail of the increasing roughness of the crack path with increasing cycles of CA at  $R=0.8$  in 'A',  $\Delta K \sim 1.5 \text{ MPa}\sqrt{\text{m}}$ . 'B' shows an example of a fracture surface produced by the spectrum (similar  $\Delta K$ ). The CA/VA spectrum is shown in the insert.

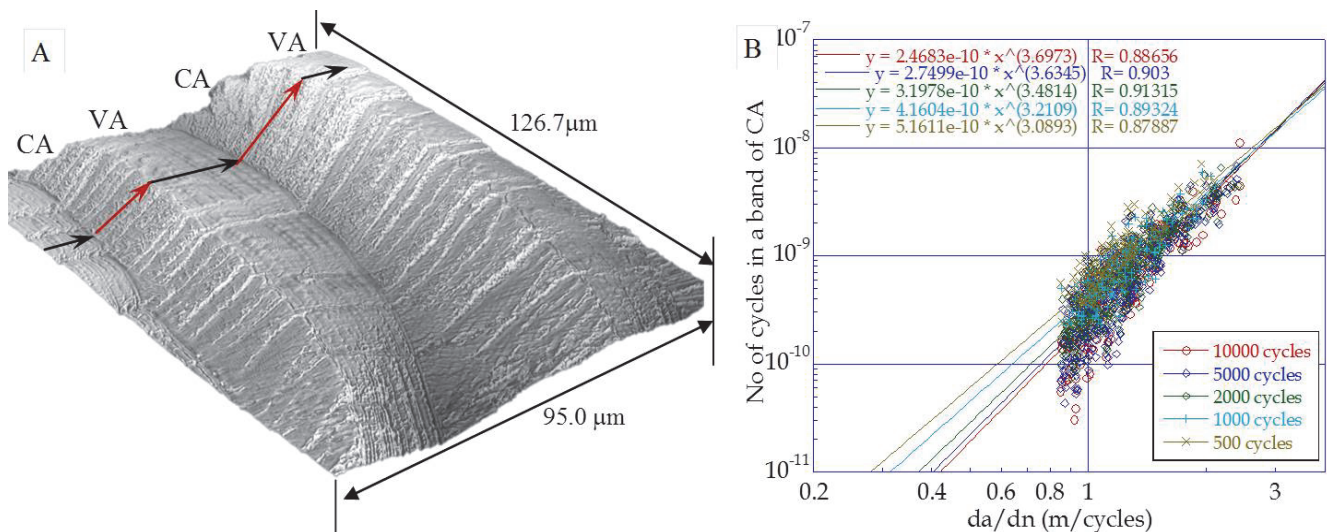


Figure 8: 'A' shows a 3D image taken of a  $0.1\text{mm} \times 0.1\text{mm}$  section from a coupon tested with CA/VA spectrum (Fig. 8) showing crack path changes between CA and VA crack growth. 'B' shows a summary of the measured crack growth rates from CA loading sub-blocks with varying cycles [24], suggesting that for growth below  $\sim 2 \times 10^{-8} \text{ m/cycle}$  the growth rates are inversely dependent on the number of CA cycles applied.



Measurement of the CA crack growth sub-block' widths and assuming a centre semi-elliptical surface crack geometry factor [25] allowed  $da/dN$  vs  $\Delta K$  data to be determined. These data are presented in Fig. 8B where power curves were fitted to the average growth of each type of CA band. It appears that the average  $da/dN$  or crack growth per cycle varies inversely with the number of cycles in the CA blocks below  $\Delta K \sim 2.5 \text{ MPa}\sqrt{\text{m}}$  or a rate of  $\sim 2 \times 10^{-8} \text{ m/cycle}$  for this material. Comparing this data to the long crack data found in [26] indicated that  $\Delta K \sim 2.5 \text{ MPa}\sqrt{\text{m}}$  was about the region from which the *Paris regime* of the  $R=0.8$  crack growth rate starts. The inverse decay suggests that growth rates will be faster with fewer CA cycles between the VA loading below this point ( $\Delta K \sim 2.5 \text{ MPa}\sqrt{\text{m}}$ ), suggesting that when the cycles are applied as VA for small cracks, a more *efficient* crack grows. All of this growth is considerably faster with lower threshold than predicted by long crack CA data alone, for example that found in Reference [26].

## CONCLUSIONS

By adjusting the pattern of loads involving sequences of high stress ratio CA cycles followed by; underloads, bands of different stress ratio cycles or bands of VA loading, distinct fracture surface features or progression marks can be produced at very low stress intensity factor range levels. Examination of the crack paths on the fracture surfaces produced by small cracks in AA7050-T7451 found that path changes were sensitive to the crystal orientation of the grain through which the crack was growing, and by using simple loading sequences the path could be changed. This observation facilitated the measurement of crack growth rates at very low  $\Delta K$  levels.

It was also observed that CA loads of varying stress ratios in bands could progressively cause retardation of further growth. Whereas changing the loading more often increased the rate of growth measured in the CA bands. This observation may help to explain why VA loading can often result in faster crack growth than is predicted from data developed from CA tests. Since for any sequence of CA loading the crack will prefer to grow on one particular plane in one direction through a grain, it was postulated that a decrease in crack growth rate could be expected particularly when the preferred local plane and direction is not aligned to the preferred average growth plane. Using VA loads results in growth that was less governed by this limitation and as such allowed growth closer to a preferred growth plain making the cracking more efficient in the small to intermediate crack regime where  $K_{max}$  is  $<$  about  $5 \text{ MPa}\sqrt{\text{m}}$ .

## ACKNOWLEDGMENTS

M. Jones, DSTO, and T. Hattenberg of NLR, are acknowledged for some of the fractography and measurement work.

## REFERENCES

- [1] White, P., Barter, S. A., Molent, L. Observations of crack path changes caused by periodic underloads in AA7050-T7451. *International Journal of Fatigue*, 30 (2008) 1267-1278.
- [2] Dainty, R. V., The use of 'marker-loads' as an aid in quantitative fractography in full-scale aircraft fatigue testing – a case study. Technical Report LTR-ST-1374. National Research Council, Canada, (1982).
- [3] Barter, S. A., Wanhill, R. J. H. Marker Loads for Quantitative Fractography (QF) of Fatigue in Aerospace Alloys, NLR Client report NLR-TR-2008-644. National Aerospace Laboratory, NLR., Amsterdam The Netherlands, (2008).
- [4] Wanhill, R. J. H., Damage tolerance engineering property evaluation of aerospace aluminium alloys with emphasis on fatigue crack growth. Technical Report NLR TP 94177U, National Aerospace Laboratory NLR; (1995).
- [5] Wallbrink, C., Jackson, P. Hu, W., Crack growth rate curves: Which Part Dominates Life Prediction and When? In: *International Committee on Aeronautical Fatigue*, Montreal, Canada, (2011).
- [6] Blom, A. F., Relevance of short crack growth data for durability and damage tolerance analysis of aircraft. *Proceedings of the Second Engineering Foundation International Conference/Workshop on Small Fatigue Cracks*, Metallurgical Soc. Inc, (1996) 623-638.



- [7] Molent, L., Barter, S. A. A comparison of crack growth behaviour in several full-scale airframe fatigue tests. *Int. Journal of Fatigue*, 29(6) (2007) 1090-1099.
- [8] ASTM E647-13a - Standard Test Methods for Measurement of Fatigue Crack Growth Rates, ed.: Am. Soc. Testing Mats., (2014).
- [9] Edwards, P., Newman, J., Short-Crack Behaviour in Various Aircraft Materials, NATO, AGARD-R-767, (1990).
- [10] Elber, W., The significance of fatigue crack closure. ASTM STP486 American Society for Testing and Materials, West Conshohocken, Pennsylvania, USA, (1971) 230-242.
- [11] Suresh, S., *Fatigue of Materials*, 2nd ed. Cambridge: Cambridge University Press, 14 (1998).
- [12] Wanhill, R. J. H., Barter, S., Molent, L., *Fracture Mechanics in Aircraft Failure Analysis: Uses and Limitations*, *Eng. Failure Anal.*, 35 (2013) 33-45.
- [13] McMillam, J. C., Pelloux R. M. N. Fatigue crack propagation under program and random loads. *Fatigue crack propagation*, ASTM STP, Am. Soc. Testing Mats., (1967) 505-535.
- [14] van der Linden, H. H., Modifications of flight-by-flight load sequences to provide for good fracture surface readability. In: *Fatigue crack topography*. AGARD conference proceedings, (1984) 376.
- [15] Forsyth, P. J. E., A two stage process of fatigue crack growth. In *Crack Propagation: Proc. of Cranfield Sym.* London: Her Majesty's Stationery Office, (1962) 76-94.
- [16] White, P., Barter, S. A., Wright, C. Small crack growth rates from simple sequences containing underloads in AA7050-T7451, *Journal of Fatigue*, 31 (2009) 1865-1874.
- [17] Laird, C., Smith, G.C., Crack propagation in high stress fatigue, *Phil Mag.*, 7 (1962) 847-857.
- [18] Pelloux, R. M. N., Crack extension by alternating shear, *Eng Fract Mech*, 1 (1970) 697-704.
- [19] Abelkis, P. R. A., Study of fatigue crack propagation under spectrum loading through the use of microfractography, In: *Fatigue of structures*, New Orleans (LA), (1975) 17-20.
- [20] Suresh, S., Ritchie, R. O., Propagation of short fatigue cracks. *International Metals Reviews*, Elsevier, 29 (1984) 445-476.
- [21] Krkoska, M., Barter, S.A., Alderliesten, R.C., White, P., Benedictus, R., Fatigue crack paths in AA2024-T3 when loaded with constant amplitude and simple underload spectra, *Engineering Fracture Mechanics*, 77(11) (2010) 1857-1865.
- [22] Ulmer, D. G, Altstetter, C. J., Hydrogen-induced strain localization and failure of austenitic stainless steels at high hydrogen concentrations, *Acta Metall Mater*, (1991) 1237-1248.
- [23] Suresh, S., Crack deflection: implications for growth of long and short cracks. *Metallurgical Transactions*, 14A (1983) 2375-2385.
- [24] Burchill, M., Barter, S., Jones, M., The effect of crack growth retardation when comparing constant amplitude to variable amplitude loading in an aluminium alloy. *Advanced Materials Research*, 891-892 (2014) 948-954.
- [25] Murakami, Y., Editor in-chief, *Stress intensity factors handbook*, Pergamon Press. (1986) 709.
- [26] Harter, J. A. AFGROW Users Guide and Technical Manual, Air Vehicles Directorate, Air Force Research Laboratory, WPAFB OH USA AFRL-VA-WP-TR-206, (2006).